MHK TURBINE THEORETICAL DESIGN

Bryan Szloh
MSME Student, Cleveland State University

Annie Poluse
MSME Student, Cleveland State University

ABSTRACT

Different types of marine hydrokinetic turbines were researched and an axial flow design that was presented in a paper by A.S Bahaj, W.M.J. Batten and G. McCann [1] was selected for a theoretical installation at a location around the Hawaiian island of Oahu. Since there are only a handful of marine hydrokinetic (MHK) turbines installed in the world, our project sought to find a new site that could benefit from the clean energy source that hydroelectric power generation provides. The site was also selected based upon the availability of surface velocity data, optimal current velocity for turbine operation, relative proximity to the shore, and location in the United States. The experimental Coefficient of Performance (C_p) and Coefficient of Thrust (C_t) curves were compared with the theoretical calculations performed in the software package AeroDyn that was provided with the software download. A point was selected that provided the maximum C_p before the onset of cavitation and was used in conjunction with the Tip Speed Ratio (λ) and Coefficient of Performance to scale the turbine to an outer blade diameter of 18 m. Our results were compared with the scaling done in the paper by Bahaj, Batten, and McCann. A theoretical power output and turbine RPM were obtained at a flow velocity of 1.9 m/s and compared with RPM values in various other papers for aquatic sea life safety. The turbine design is bare (no duct) and is a floating design to capture the higher current velocities near the top of the boundary layer. This mini project was done to fulfill the requirements of a graduate level Applied Fluid Mechanics course.

NOMENCLATURE, ACRONYMS, ABBREVIATIONS

A	Swept area of rotor (m^2)
C_p	Coefficient of performance
C_t	Coefficient of thrust
λ	Tip speed ratio (TSR)
ω	angular velocity (rad/s)
r	radius of blades from center of hub (m)
v	free stream velocity (m/s)
P	power (W)
ρ	density (kg/m^3) – assumed to be 1025 kg/m^3
Re	Reynolds number
σ_c	Cavitation number

INTRODUCTION AND GENERAL RELATIONS

Marine hydrokinetic (MHK) turbines are used to capture the energy of moving water much like wind turbines capture the energy of moving air. Since water is roughly 800 times denser than air, MHK turbines could potentially produce significantly more power than wind turbines. Marine turbines are mostly independent of weather, which can have a large impact of the effectiveness of other forms of renewable energy [2]. The capacity factor (actual energy output divided by the theoretical maximum power) of marine current is likely 40-50% as compared to 25-30% for wind power [2]. Tides and ocean currents provide a predictable and continuous flow of water and since water covers about 71% of the earth surface, it would seem like MHK turbines would be an excellent source of renewable energy.

The state of Hawaii has the highest electricity prices of all the states in the United States and depends more on petroleum for its energy need than any other state [17]. As of 2016, hydroelectric power generation only accounts for a small fraction of Hawaii's renewable energy source [17]. Because of this and since Hawaii is an island in the vast Pacific Ocean, an MHK turbine would be a good hydroelectric source to capture the continuous and predictable flow of the ocean current.

After researching different types of turbines (such as vertical axis, tidal barrage, and oscillating hydrofoils), we selected an axial flow horizontal axis turbine since most MHK turbines fall in this category and the most information about their design could be found.

The power output of a horizontal axis turbine can be found from the power coefficient:

$$C_p = \frac{P}{(0.5\rho A v^3)} \tag{1}$$

where P is the turbine power, ρ is the water density (1025 kg/m^3 for saltwater), A is the swept area of the rotor (= πr^2), and v is the free stream velocity.

The amount of thrust placed upon a horizontal axis turbine can be found from the thrust coefficient:

$$C_t = \frac{T}{(0.5\rho A v^2)} \tag{2}$$

where T is the turbine thrust, ρ is the water density (1025 kg/m^3 for saltwater), A is the swept area of the rotor (= πr^2), and v is the free stream velocity.

The Tip speed ratio (λ) is another useful relation that can be used to find the rotational speed of the turbine rotor and is found from:

$$\lambda = \frac{\omega r}{v} \tag{3}$$

where ω is the rotor angular velocity, r is the radius of the rotor blades, and v is the free stream velocity.

Lastly, the cavitation number is found from:

$$\sigma_c = \frac{(P_{atm} + \rho g H) - P_v}{0.5\rho U^2} \tag{4}$$

where P_{atm} is the atmospheric pressure, g is the gravitational force, H is the height below the water surface, P_v is the vapor pressure of the fluid and U is the fluid velocity on the blade section.

TURBINE SITE SELECTION

The range of marine currents that are usable with MHK turbines falls within 1 to 4 m/s with the target marine current having an average velocity of 2.5 m/s [2]. Keeping this in mind, a search for a location that came as close as possible to the target flow rate of 2.5 m/s was done. We found a location that is roughly 100 km off the coast of Honolulu in the North Pacific Ocean using the Coastal Observing Research and Development Center website [3]. A screenshot of our exact location is shown below in Figure 1.

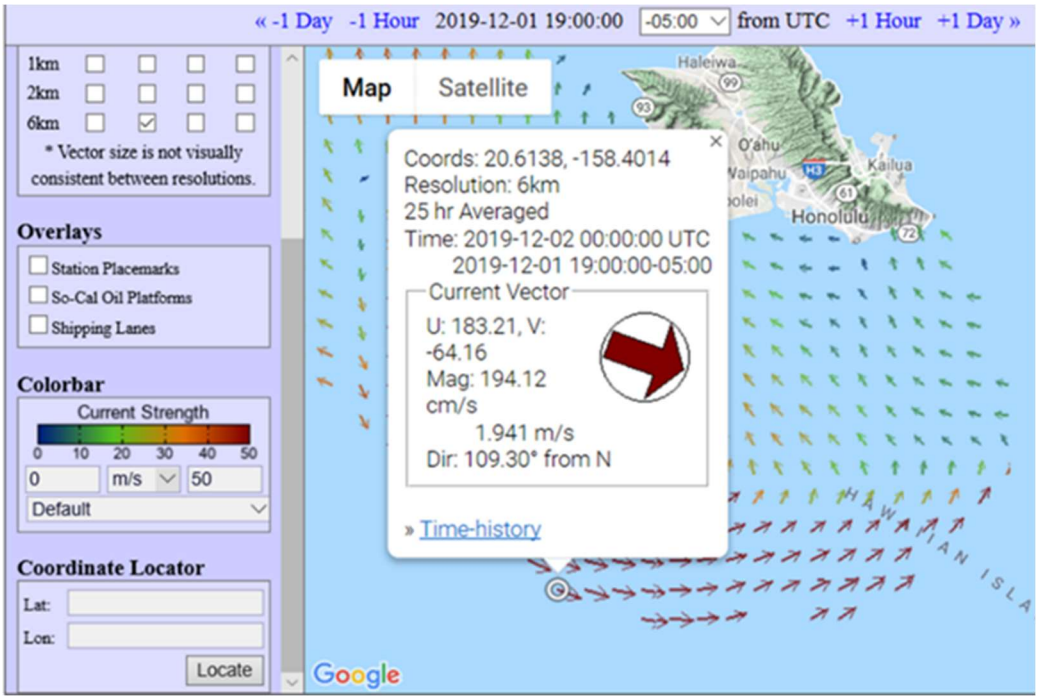

Figure 1. Coastal Observing Research and Development Center website location information.

The surface velocity is showing 1.941 m/s at the location. The coordinates of the location (20.6138, -158.4014) were input into Google Maps [4] and a depth of about 4570 m was found at this point as shown in Figure 2.

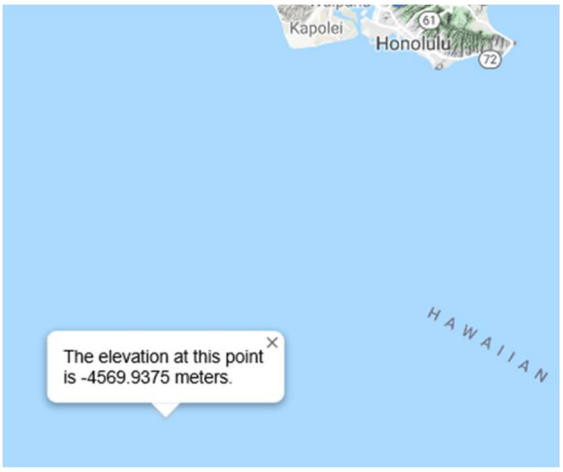

Figure 2. Depth of ocean at location from Google Maps.

Using the data from the site, we came up with a velocity profile using h = 4500 m and $U_{max} = 1.9\ m/s$ for a power law profile and parabolic profile (for comparison) of the boundary layer as shown in Figure 3.

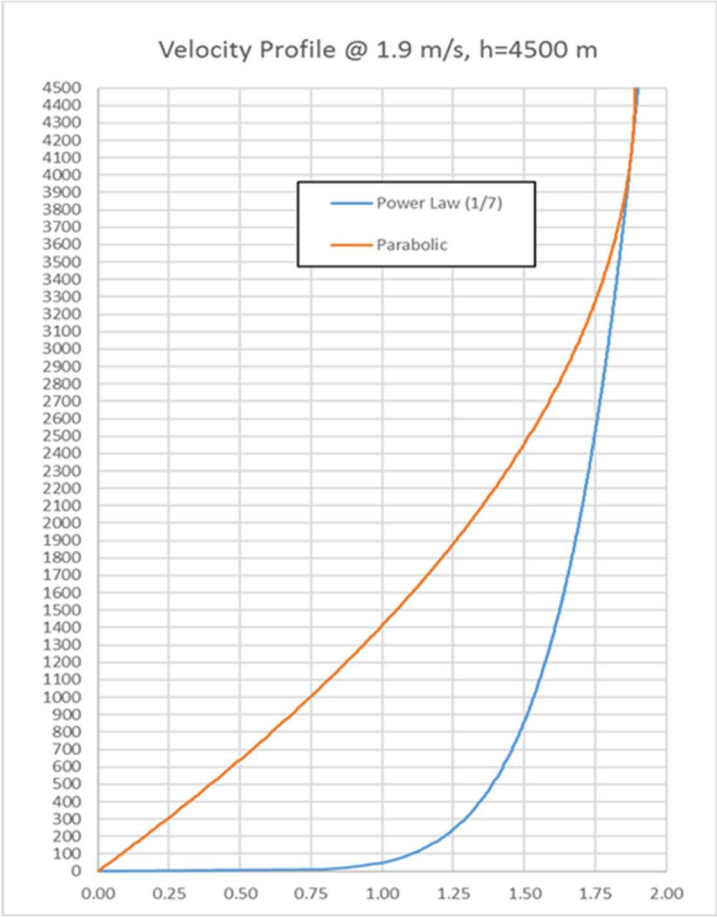

Figure 3. Power law and Parabolic Velocity Profile of Boundary Layer at Location.

Equations 5 and 6 were used to determine the Power Law and Parabolic velocity profiles respectively.

$$U(h) = 1.615\left[\frac{h}{(0.32)(4500)}\right]^{\frac{1}{7}} \tag{5}$$

$$U(h) = 0.00042\left[\frac{h^2}{4500} - 2h\right] \tag{6}$$

It can be seen from Equation 5 that the 1/7 power law was used and a bed roughness value of 0.32 was assumed which corresponds to a typical value used in shelf-sea oceanographic research [5]. Data from measurements made using an Acoustic Doppler current profiler (ADCP) at the location would yield a more realistic velocity profile.

DESIGN METHOD OVERVIEW

A common analytical method used in hydrodynamic design of turbine blades is Blade Element Momentum (BEM) Theory. BEM is an analytical model that iterates between Momentum Theory (used to derive the axial and circumferential inflow factors) and Blade Element Theory (used to model the section drag and torque) [6]. The blade is divided into elements along the length and 2D aerodynamic forces and moments are calculated at nodes (one node per element) as distributed loads per unit length using and annular control volume; loads are then integrated over the blade length to approximate 3D loads over the entire blade [6]. The positives of this method are that BEM models are fast and efficient; thus a large number of trials can be run [6], however, they are not accurate for estimation of wake effects, complex 3D flow or dynamic stall, and chordwise loading.

The software package, AeroDyn [7], was evaluated in Matlab for the design of turbines and uses BEM theory to calculate the Coefficient of Performance and Coefficient of Thrust vs. Tip Speed Ratio curves for a given turbine and can perform a cavitation check at each node for each TSR iteration step. It requires four input files: the main driver file, the primary input file, the blade geometry file, and the airfoil data file. The blade geometry file and airfoil data file can be generated from an airfoil design program such as XFOIL. Included in the software download was a file that contained the test data and input files of the 0.8 m diameter turbine that was designed and then tested in a cavitation tunnel and tow tank by Bahaj, Batten, and McCann [1] that we will use as our model turbine.

TURBINE SIZING AND SCALING

AeroDyn was then run with the input files based upon the tests done on the turbine by Bahaj, et al. and the following curve was generated as shown in Figure 4.

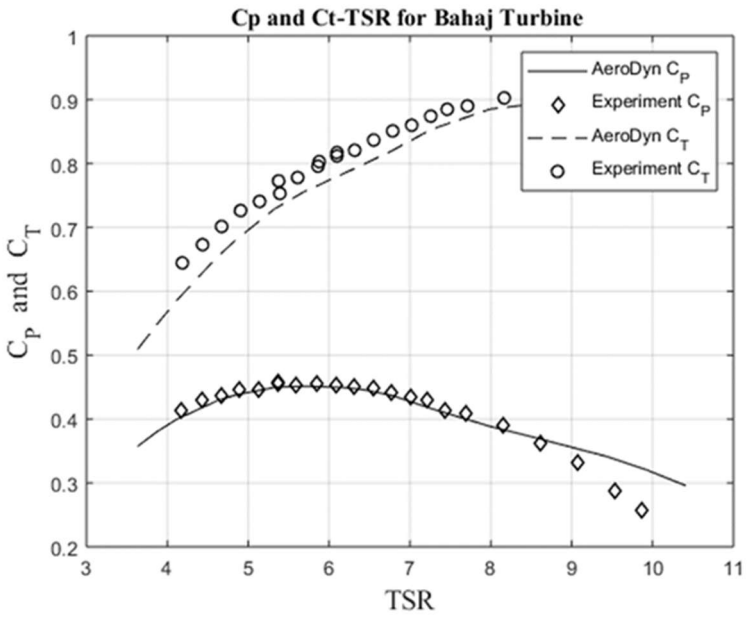

Figure 4. Performance curve generated using AeroDyn for 0.8 m dia. turbine data with plot of test data.

The Coefficient of performance curve was then evaluated along with the results data from Matlab to find the highest Coefficient of Performance before the onset of cavitation. This corresponded to a TSR of 4.8425 at a C_p of 0.4377. The TSR and corresponding C_p were then used to determine the estimated power generated using Equation 1 and an estimated turbine rpm using Equation 3. The results from the AeroDyn curve and measurements taken of the 0.8 m turbine scaled up to a 20m diameter at a 2.5 m/s free stream velocity are summarized below in Table 1.

Table 1. AeroDyn curve vs. measured data curve turbine scaling.

	AeroDyn curve	Experiment curve [1]
TSR	4.8425	6
C_p	0.4377	~0.46
P	1.16 MW	1.13 MW

It can be seen that the AeroDyn simulation came within 2.65% of the results based on a spline fit of the 0.8 m diameter turbine test results. This would indicate that the method of estimation based on an AeroDyn generated curve is a good approximation that can be used to accurately estimate the power output of the scaled-up model turbine.

It was decided to use a slightly smaller scaled up version of the model turbine for our installation at our site off the coast of Oahu. An 18 m diameter turbine would be chosen and based upon a free stream velocity of 1.9 m/s, we came up with an estimated power output of 392 kW rotating at 9.76 rpm. A floating platform design was chosen as this type seems to be suited for deep water installations [2] and is pictured below with other types in Figure 5.

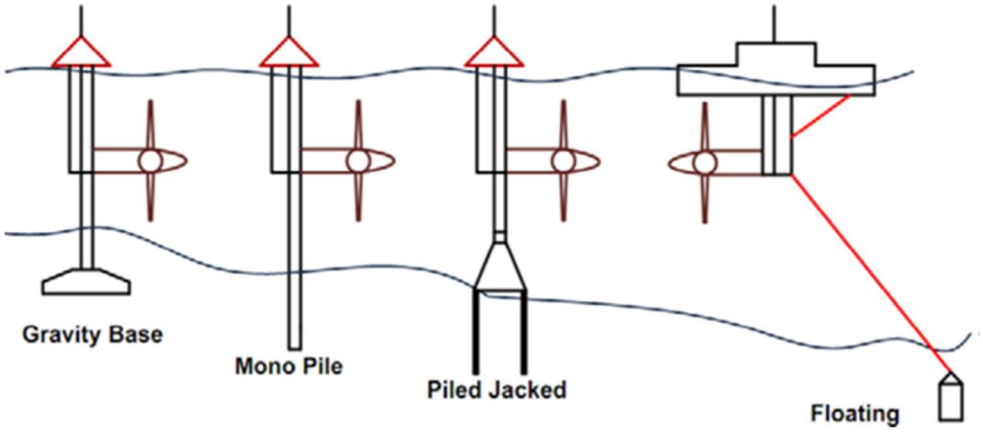

Figure 5. Types of axial flow turbine mountings.

Also, the floating platform design would allow the turbine to capture the maximum free stream velocity which would be nearest the top of the boundary layer or surface of the ocean stream. Since the velocity of 1.9 m/s falls within the range of recommended velocities, a duct would not be used to augment the velocity of the free stream.

ENVIRONMENTAL CONSIDERATIONS

Interaction with aquatic wildlife and ocean floor

Consideration needs to be taken to avoid harming any potential wildlife that may be in the proximity of the turbine. The Pacific Ocean near Hawaii is home to many unique forms of ocean life including several endangered species such as the Hawaiian monk seal and green sea turtle. Therefore, some research was done to find the results of any types of studies done on the effects of axial flow turbines and wildlife. Two such studies were found that involved simulations with fish. The first study done by Zhang et al [8] used a 1:100 scale turbine with a TSR of 5 and blade diameter of 25 cm in a tank using live fish ranging from 3 to 4.2 cm long. The flow velocity was set at 5 cm/s and turbine rpms of 0, 5, and 20 were considered. The results showed that no fish were observed to contact or collide with the turbine in the experiment. A second study was done by Romero-Gomez and Richmond [9] where a simulation using a 3 bladed turbine with blade radius of 2.44 m with fish sizes ranging from 100 to 760 mm with a free stream velocity of 1, 2, and 3 m/s (corresponding to TSR of 8, 4, and 2.67) showed that a low mortality rate was found (<4%) which is consistent with previous experimental observations. The results of these studies seem to indicate that an axial flow turbine would have little effect on fish in the area, however, consideration needs to be taken for other types of wildlife. Also, the floating type configuration would keep the turbine far from the ocean floor where the wake might cause the sediment on the ocean floor to be disturbed.

Elimination of potential leak paths

The elimination of lip seals in the design of the turbine nacelle on the turbine shaft would eliminate any possibility of leaking a petroleum-based lubricant into the ocean. Incorporating

the magnetic coupling design as shown by Tian et al [10] between the turbine shaft and gearbox in the nacelle along with permanently sealed bearings would alleviate any type of lubricant leakage potential from the gearbox as the gearbox end would be completely enclosed by an isolation hood.

Reduction in noise generated by turbine

The noise generated by the turbine in the water will also need to be evaluated. Cavitation produces unnecessary noise and eliminating this will be a good start to minimizing the noise the turbine blades produce. A gearbox that reduces noise such as one that uses helical gears could be utilized, however, helical gears are not as efficient at transmitting power as spur gears.

DISCUSSION OF TURBINE DUCTS

A duct on a turbine acts as a type of nozzle that increases the incoming velocity of the fluid to the entrance of the turbine that allows the turbine to rotate at a higher rpm and thus produce more power. A simple Bernoulli equation analysis of the entrance and exit of the turbine duct yields Equations 7 and 8 shown below:

$$V_2 = V_1 \frac{A_1}{A_2} \tag{7}$$

$$P_2 = P_1 + \frac{1}{2} \rho \, (V_1^2 - V_2^2) \tag{8}$$

where P_1, V_1, and A_1 are the entrance pressure, velocity, and area and P_2, V_2, and A_2 are the exit pressure, velocity, and area and shows that an increase in velocity of a fluid will also result in a decrease of the fluid pressure. Decreasing the fluid pressure at the entrance to the turbine could result in a decrease in the cavitation number which could result in a better chance of cavitation occurring. Also, cavitation is more likely to occur near the surface of the ocean since the static pressure term of the cavitation number decreases, thus resulting in decreased cavitation number. Lastly, the performance increase with a duct does not seem to have a significant impact. In a study done by Mohammed et al [11] on a 20 m diameter turbine, only a 3.67% to 5.30% maximum increase in performance was calculated with using a duct. In order to avoid cavitation issues with the turbine, the design does not include a duct.

SUGGESTIONS FOR FURTHER INVESTIGATION

Design of Floating Platform

The final mass of the submerged turbine structure needs to be determined as well as an estimate of the thrust force from the coefficient of thrust in order to begin to design a floating platform for the turbine. The buoyancy of the submerged turbine structure (if any) and that of the floating platform need to be determined. If the turbine platform is to be affixed to the ocean floor with cabling, the weight of the structural cabling as well as the electrical cabling that connects the turbine to the grid needs to be considered. The normal weather conditions and

wave height need to be considered as well as any type of catastrophic event such as a hurricane. The steadiness of the flow direction needs to be monitored and if it is unsteady, a system that accounts for the changing direction of flow can be designed into the platform [12].

Design of method to affix platform to ocean floor and mooring

An actual assessment needs to be made of the type of rock on the ocean floor at the location so that moorings can be designed and installed. These moorings need to be able to withstand the loading from the floating platform cables under normal and catastrophic weather conditions or a type of breakaway system needs to be designed that would allow the turbine to disconnect from its structural and electrical cabling during catastrophic events. Golightly [13] outlines various methods of mooring and anchoring a wind turbine to the seafloor, similar methods can be used for an axial flow water turbine.

Design of gearbox and generator

The gearbox needs to handle the load from the turbine, have adequate torque capacity, have the needed output rpm to meet the input rpm requirements to drive the generator, and possess a relatively long life to keep ongoing maintenance costs down. Gearbox temperature needs to be considered as well as a suitable heat transfer system to maintain the gearbox lubricant temperature to an acceptable level. The ocean itself could provide an adequate heat sink for this.

Tian et al [10] makes use of a permanent magnet DC generator manufactured by Maxon and uses an isolation hood with a rare earth magnetic coupling as mentioned above to avoid seal friction. Beam et al [15] describes the design of the whole power-take-off of a 0.55 MW MHK turbine designed for use in Puget Sound, WA, USA; the system uses a cartridge seal (about 20 year life with 2 year maintenance interval for grease injection) for drivetrain isolation from the seawater and describes in detail the components used using as much COTS (commercially available off the shelf) components as possible. It too uses a permanent magnet DC generator along with a planetary gearbox to increase rather than decrease the shaft rpm to the generator.

Electrical system, cabling, and connection to grid

The design of a transmission system as well as an economic assessment of a MHK turbine is found in Li et al [14] and in the supplement.

Stress (FEA) Analysis of turbine blades

Once a final blade material is selected (if different than solid aluminum since materials such as titanium, stainless steels, nickel-copper alloys and high-nickel alloys can highly reduce or eliminate corrosion [2]) a stress analysis needs to be done. The turbine design software HarpOpt (available from the NREL website) will evaluate the stresses on the turbine blades and come up with an optimal design. The pressure data at each node from a BEM analysis could be used as an input file to a commercial FEA package and used to analyze the stresses on the turbine blades as well. Mohammed et al [11] used a panel method to perform a hydrodynamic

analysis of the Bahaj turbine to obtain the hydrodynamic pressure and used this as the input to the structural FEA code.

Final power output estimation

The calculation of 392 kW from the 18 m diameter turbine represents the theoretical resource available from the turbine [12]. The technical resource which is the energy that can be extracted by present HEC technology and the practical resource which is the energy that can be extracted considering all practical factors must be considered for a more realistic estimate of the turbine output at its proposed location [12].

Gearbox efficiency, generator efficiency, transmission losses, and variability in the free stream velocity need to be accounted for. A paper by Domenech et al [15] discusses a method of assessing a practical value of energy extraction from a turbine using NOAA CO-OPS' Mapping and Charting Services Program data.

Maintenance Considerations

The development of sensors to monitor the health of the turbine and act as a predictive maintenance system needs to be designed to alert operators to a maintenance need or of any type of changing operational condition [12]. Blade soiling and fouling is another maintenance issue that needs to be addressed as this will tend to reduce the power coefficient [12]. Access to the turbine by an ocean going vessel or from an offshore platform should be planned for, however, the system should only require a minimum level of maintenance [2].

CONCLUSIONS

In conclusion, we were able to research the various types of turbines, the parameters that need to be considered in their design, and the various methods used to design a marine hydrodynamic turbine. With this information, a site was selected (off the coast of the Hawaiian island of Oahu) that was a good candidate for a new turbine installation that would provide a clean source of energy; a turbine type was chosen and an existing design was scaled to fit the location that was selected. We were also able to become familiar with the BEM theory turbine design package AeroDyn. Overall, we gained a good knowledge of the foundations of MHK turbine design as well as some of the current technologies that are in use on existing turbine installations. We hope that this paper will serve as a contribution to another potential MHK turbine site in the United States and to help Hawaii in identifying and implementing another clean and economical energy source.

APPENDIX A

Below are the general specifications of the theoretical turbine design.

Turbine outer diameter	18	m
Theoretical power output	392	kW
Blade profile	NACA 63-8xx	-
Number of blades	3	
Set angle	5	degrees
Mounting	Floating platform type	
Blade Material	Aluminum alloy	

REFERENCES

[1] Bahaj, A.S., W.M.J. Batten, and G. McCann, "Experimental verifications of numerical predictions for the hydrodynamic performance of horizontal axis marine current turbines," Renewable Energy, Vol. 32, 2007, pp. 2479 – 2490.

[2] Chen, Hao, Tianhao Tang, Nadia Ait-Ahmed, Mohamed El Hachemi Benbouzid, Mohamed Machmoum, and Mohamed El-Hadi Zaim, "Attraction, Challenge and Current Status of Marine Current Energy," IEEE Access, Vol. 6, 2018, pp. 12665 – 12685.
doi: 10.1109/ACCESS.2018.2795708

[3] Coastal Observing Research and Development Center:
http://cordc.ucsd.edu/projects/mapping/maps/

[4] Google Maps; Elevation Service: https://developers-dot-devsite-v2-prod.appspot.com/maps/documentation/javascript/examples/elevation-simple

[5] Lewis, M. S.P. Neill, P. Robins, M.R. Hashemi, and S. Ward, "Characteristics of the velocity profile at tidal-stream energy sites," Renewable Energy, Vol. 114, 2017, pp. 258-272.

[6] Murray, Robynne, "Predicting Cavitation on Marine and Hydrokinetic Turbine Blades with AeroDyn V15.04", NREL/TP-50000-68398, August 2017.

[7] AeroDyn, Axial Flow Turbine Design, Aerodynamics module software, Ver. 15.04, National Renewable Energy Laboratory, Golden, CO, April 2017.

[8] Zhang, Jumbo, Daisuke Kitazawa, Sayuri Taya, and Yoichi Mizukami, "Impact assessment of marine current turbines on fish behavior using an experimental approach based on the similarity law," Journal of Marine Science and Technology, Vol. 22, 2017, pp. 219-230.
doi: 10.1007/s00773-016-0405-y

[9] Romero-Gomez, Pedro, and Marshall C. Richmond, "Simulating blade strike on fish passing through marine hydrokinetic turbines," Renewable Energy, Vol. 71, 2014, pp. 401-413.

[10] Tian, Wenlong, Zhaoyong Mao, and Hao Ding, "Design, test and numerical simulation of a low-speed horizontal axis hydrokinetic turbine," International Journal of Naval Architecture and Ocean Engineering, Vol. 10, 2018, pp. 782-793.
doi: 10.1016/j.ijnaoe.2017.10.006

[11] Mohammed, Mahrez Ait, Mostapha Tarfaoui, Jean Marc Laurens, and Sylvain Moyne, "Design of Composite Ducted Horizontal Axis Turbine," VI International Conference on Computational Methods in Marine Engineering, 2015, Rome, Italy, pp. 1-22.

[12] Laws, Nicholas D., and Brenden P. Epps, "Hydrokinetic energy conversion: Technology, research, and outlook," Renewable and Sustainable Energy Reviews, Vol. 57, 2016, pp. 1245-1259.
doi: 10.1016/j.rser.2015.12.189

[13] Golightly, Chris, "Anchoring and Mooring for Floating Offshore Wind", OSIF Meeting, Fugro Nootdorp, NL, Nov 2018.

[14] Li, Binghui, Anderson Rodrigo de Queiroz, Joseph F. DeCarolis, John Bane, Ruoying He, Andrew G. Keeler, and Vincent S. Neary, "The economics of electricity generation from Gulf Stream currents," Energy, Vol. 134, 2017, pp. 649 – 658
doi: 10.1016/j.energy.2017.06.048

[15] Domenech, John, Timothy Eveleigh, and Bereket Tanju, "Marine Hydrokinetic (MHK) systems: Using systems thinking in resource characterization and estimating costs for the practical harvest of electricity from tidal currents," Renewable and Sustainable Energy Reviews, Vol. 81, 2018, pp. 723 – 730
doi: 10.1016/j.rser.2017.07.063

[16] Beam, M., B. Kline, B. Elbing, W. Straka, A. Fontaine, M. Lawson, Y. Li, R. Thresher, and M. Previsic, "Marine Hydrokinetic Turbine Power-Take-Off Design for Optimal Performance and Low Impact on Cost-of-Energy," National Renewable Energy Laboratory, CP-5000-58092, February 2013.

[17] "Hawaii Energy Facts and Figures," Hawaii State Energy Office, May 2017